CAV2021
11th International Symposium on Cavitation
May 10-13, 2021, Daejon, Korea

A Model for a Laser-induced Cavitation Bubble

Xiaoxu Zhong [1], Javad Eshraghi [1], Pavlos Vlachos [1], Sadegh Dabiri [1] and Arezoo M. Ardekani [1]*

[1]School of Mechanical Engineering, Purdue University, USA

Abstract: Cavitation bubbles can be generated by a laser or acoustic waves in experiments. In experiments of laser-induced cavitation, the nucleation site and its position are accurately controlled, and the induced bubble is approximately spherical. However, the complex mechanism behind the laser-induced cavitation bubble leads to challenges in its modeling. Current models can only well predict the radius of the single laser-induced cavitation bubble for one or two cycles. To fill the gap, we propose a new model which takes into account the liquid compressibility, heat transfer, and non-equilibrium evaporation and condensation. Specifically, we use a new approximation of the temperature gradient at the bubble surface. Similar to other models, our model has several unknown physical parameters, including the initial number of air / vapor molecules, the evaporation coefficient, and the initial thermal layer thickness in the bubble. We adopt a Bayesian approach to fit the experimentally measured bubble radii such that we obtain the probability distributions, rather than point estimates, of the unknown parameters. Experimental data of bubble radii are in the 95% confidence interval of our model prediction. The variabilities of the peak pressure and temperature are large, which partly explains why different values (even different magnitudes) of peak pressure and temperature are reported in the literature.

Keywords: Laser-induced cavitation bubble; evaporation and condensation; heat transfer

1. Introduction

Cavitation occurs when the pressure in the liquid drops below the vapor pressure. The violent collapse of the cavitation bubble induces high temperature and pressure around the bubble surface with the emission of shock waves. If the bubble is close to a solid, the collapse of the bubble also generates a high-speed jet toward the solid surface. The generated shock wave and high-speed jet are strong enough to rupture the membrane of the cell [1], clean the surface of solids, and even break the ice [2]. There are extensive studies on the dynamics of a cavitation bubble [3-5], but the complex physics behind the cavitation bubble leads to challenges in its modeling. Fujikawa and Akamatsu [6] presented a detailed analysis for the laser-induced cavitation bubble. Their results indicate that evaporation and condensation have a significant impact on bubble dynamics. Also, increasing the air content of the bubble reduces the peak pressure and temperature [6]. Yasui [7] developed a simple model for the acoustic cavitation bubble. This model can reduce to a set of first-order equations, which can be solved by the explicit Euler method.

We modified the model, which was originally proposed by Yasui [7] for acoustic-induced cavitation bubbles, to account for the dynamics of the laser-induced cavitation bubble [8]. The predicted bubble radii agree with the experimental measurements within 10% for several cycles of bubble growth and collapse. However, there are four unknown parameters in our model which are determined by fitting the experimentally measured bubble radii. The four unknown parameters have a significant effect on the peak pressure and temperature [8]. In this paper, we use a Bayesian model calibration [9], to find the probability distributions, rather than point estimates, of the four unknown parameters. This is logically rigorous since 1) there are multiple combinations of unknown parameters that lead to the minima of the loss function; 2) point estimates always deviate from the exact values of the unknown parameters, which depends on

---

* Corresponding Author: Arezoo M. Ardekani, ardekani@purdue.edu

the amount of available experimental data. However, the frequentist inference cannot characterize the deviation; 3) the results predicted by the Bayesian approach is more reliable than those by frequentist inference for outliers. Experimentally measured bubble radii are in the 95% confidence interval of our model prediction, but our results indicate large variabilities in the peak pressure and temperature. Most models for the laser-induced cavitation fit the experimental data of bubble radii to obtain the values of unknown physical parameters, and this is the reason different values (even different magnitudes) of the peak pressure and temperature are reported in literature.

2. Model

Our model for the laser-induced cavitation bubble is shown in Figure 1. Following assumptions are used: 1) The bubble is spherical with a uniform pressure inside it. 2) There are two thermal layers around the bubble surface. 3) Thermal conduction, evaporation, and condensation occur in the thermal layer I with a thickness δ_I, which is inside the bubble. 4) Thermal conduction occurs in the thermal layer II with a thickness δ_{II}, which is in the liquid. 5) There is a temperature discontinuity at the bubble surface. 6) The temperature profile in the thermal layer II is a parabolic curve [6]. 7) The thickness of the thermal layer II is inversely proportional to the square of the bubble radius.

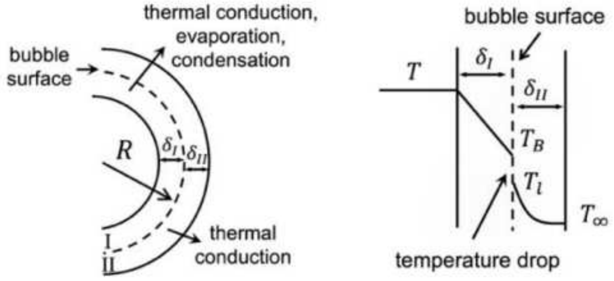

(**a**) (**b**)

Figure 1. (**a**) Thermal conduction, evaporation, and condensation occur in the thermal layer I. Thermal conduction occurs in the thermal layer II; (**b**) There is a temperature discontinuity at the bubble surface.

We use the modified Rayleigh-Plesset equation [6]

$$R\left(\ddot{R}-\frac{\ddot{m}}{\rho_l}\right)\left[1-\frac{1}{c}\left(2\dot{R}-\frac{\dot{m}}{\rho_l}\right)+\frac{1}{c^2}\left(\frac{23\dot{R}^2}{10}-\frac{31\dot{m}\dot{\rho}}{10\rho_l}-\frac{\dot{m}^2}{5\rho_l^2}\right)\right]+\frac{3}{2}\left(\dot{R}-\frac{\dot{m}}{\rho_l}\right)\left[\dot{R}+\frac{\dot{m}}{3\rho_l}-\frac{4\dot{R}^2}{3c}+\frac{1}{c^2}\left(\frac{7\dot{R}^3}{5}-\frac{49\dot{m}\dot{R}^2}{30\rho_l}-\frac{14\dot{m}^2\dot{R}}{15\rho_l^2}-\frac{\dot{m}^3}{6\rho_l^3}\right)\right]$$
$$+\frac{p_\infty-p_{B,2}}{\rho_l}-\frac{R\dot{p}_{B,1}}{\rho_l c}+\frac{1}{\rho_l c^2}\left[R\dot{p}_{B,1}\left(2\dot{R}-\frac{\dot{m}}{\rho_l}\right)+\left(p_\infty-p_{B,1}\right)\left(\frac{\dot{R}^2}{2}-\frac{3\dot{m}\dot{R}}{2\rho_l}-\frac{\dot{m}^2}{\rho_l^2}+\frac{3p_\infty-3p_{B,2}}{2\rho_l}\right)\right]=0, \qquad (1)$$

in which

$$p_{B,1}=p-\frac{2\sigma}{R}-\frac{4\mu}{R}\left(\dot{R}-\frac{\dot{m}}{\rho_l}\right)-\dot{m}^2\left(\frac{1}{\rho_l}-\frac{1}{\rho_g}\right), \quad p_{B,2}=p_{B,1}+\frac{4\mu}{3c^2}\left[\frac{3\dot{m}}{2\rho_l R}\left(\dot{R}-\frac{\dot{m}}{\rho_l}\right)^2-\frac{\dot{p}_{B,1}}{\rho_l}+\frac{\dot{m}\left(p_\infty-p_{B,1}\right)}{\rho_l^2 R}\right]. \qquad (2)$$

R, c, ρ_l, σ, μ, p, p_∞, $\dot{m}$, and ρ_g are the radius of the bubble, the speed of sound in the liquid, the liquid density, the surface tension coefficient, the liquid viscosity, the pressure inside the bubble, the pressure in the liquid at infinity, the net evaporation rate, and the average density inside the bubble, respectively. We apply the Van der Waals equation, $(p+a/v^2)(v-b)=R_gT$, for the mixture of air and vapor inside the bubble [7]. a, b, T, R_g, and v are the coefficient of the intermolecular attraction of air, the volume occupied by vapor molecules, the temperature inside the bubble, gas constant, and the molar volume, respectively.

The net evaporation rate, $\dot{m}$, is expressed by the modified Hertz-Knudsen-Langmuir relation, $\dot{m}=\dot{m}_{eva}-\dot{m}_{con}$, where the evaporation rate $\dot{m}_{eva}=\alpha_M p_v^*(T_l)/\sqrt{2\pi R_v T_l}$, and the condensation rate $\dot{m}_{con}=$

* Corresponding Author: Arezoo M. Ardekani, ardekani@purdue.edu

$\alpha_M \Gamma p_v/\sqrt{2\pi R_v T_B}$. α_M, R_v, $p_v^*(T_l)$, T_B, and T_l are the evaporation coefficient, gas constant of the vapor, saturated vapor pressure, vapor temperature at the bubble surface, and the liquid temperature at the bubble surface, respectively. Γ is a correction factor for the non-equilibrium evaporation and condensation process, its expression can be found in [8]. The changes in the number of vapor and air molecules are

$$\dot{n}_{vapor} = 4\pi R^2 \dot{m} N_A / M_{vapor}, \qquad \dot{n}_{air} = 4\pi R D (c_0 - c_s), \tag{3}$$

where M_{vapor} is the molar weight of vapor, D is the diffusion coefficient of air in the liquid, c_0 is the number concentration of air in the liquid at infinity, c_s is the saturated air concentration at the bubble surface. The temperature discontinuity at the bubble surface is approximated as $T_B - T_l = \Lambda(\partial T_I/\partial r)|_{r=R}$, in which $(\partial T_I/\partial r)|_{r=R}$ is the temperature gradient at the bubble surface in the thermal layer I. The expression of Λ can be found in [7, 8]. We approximate $(\partial T_I/\partial r)|_{r=R}$ as $(T_B - T)R^2/\left(\delta_I^{(0)} R_0^2\right)$, where $\delta_I^{(0)}$ represents the thickness of the thermal layer I at the initial moment.

The internal energy of the bubble is $E = n_{air} e_{air}(T) + n_{vapor} e_{vapor}(T) - a(n_t/N_A)^2/V$, where V is the volume of the bubble. $e_{air}(T)$ and $e_{vapor}(T)$ are the energy carried by one air molecule and one vapor molecule at temperature T, respectively. The change of the energy inside the bubble is

$$\dot{E} = -4\pi R^2 \dot{R} p + 4\pi R^2 \left[\dot{m}_{eva} e_{vapor}(T_l) - \dot{m}_{con} e_{vapor}(T_B)\right] \frac{N_A}{M_{vapor}} + \dot{n}_{air} e_{air}(T'') + 4\pi R^2 \kappa \left.\frac{\partial T_I}{\partial r}\right|_{r=R} + \sigma_r 4\pi R^2 (T_B^4 - T^4), \tag{5}$$

where σ_r is the Stefan-Boltzmann constant. $T'' = T_l$ if $\dot{n}_{air} > 0$, otherwise $T'' = T$.

3. Results

We use the same values of the physical parameters as those in [8]. The moment when the bubble radius reaches its maximum is taken as $t = 0$. There are four unknown parameters in our model: the initial number of air and vapor molecules inside the bubble, the initial thickness of the thermal boundary layer I, and the evaporation coefficient α_M. We use a python package, namely *pymcmcstat* [9], to perform the Bayesian model calibration. The calibrated values are listed in Table 1. The experimentally measured bubble radii are in the 95% confidence interval of our model prediction, as shown in Figure 2 (a). Box plots of the peak temperature and pressure are shown in Figures 2 (b) and (c). The peak temperature and pressure spread out, which indicates a large variability in these parameters. Figure 2 (d) shows the comparison of different models and the experimental data, in which our model produces the best predictions of the bubble radii. The decrease of the number of vapor molecules inside the bubble explains the reduction of the amplitude of the bubble radius, as shown in Figure 2 (e). Figure 2 (f) shows the pressure in the liquid, p_l, during the first collapse stage. The pressure near the bubble surface increases from 200 bar at 111.75 μs to 600 bar at 111.8 μs. Thus, it is difficult to capture the exact peak pressure in the experiments.

Table 1. Calibrated values of the four unknown parameters in our model.

Parameters	Symbols	Mean values	Standard deviation	Units
Initial number of air molecules	$n_{air}^{(0)}$	1.1×10^{14}	3.1×10^{13}	-
Initial total number of molecules	$n_t^{(0)}$	3.4×10^{16}	1.0×10^{16}	-
Initial thickness of thermal layer I	$\delta_I^{(0)}$	28.5	13.4	μm
Evaporation coefficient	α_M	0.047	0.007	-

Acknowledgments: This research was supported by grants from the National Science Foundation [CBET-1705371] and the Eli Lilly and Company.

* Corresponding Author: Arezoo M. Ardekani, ardekani@purdue.edu

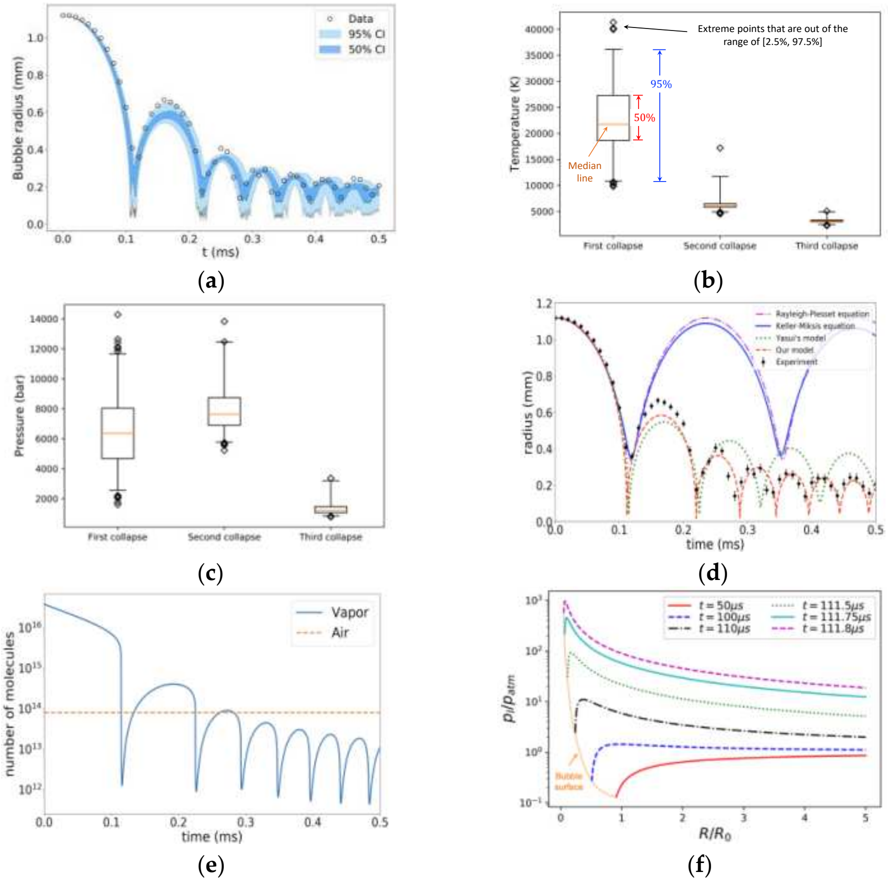

(**a**) (**b**)

(**c**) (**d**)

(**e**) (**f**)

Figure 2. (**a**) Comparison of our model prediction and experimental data from [8]; (**b-c**) The peak temperature and pressure inside the bubble. ◊: extreme points that are out of the range of [2.5%, 97.5%]; (**d**) Comparison of different models. Mean values in Table 1 are used in our model. The values of unknown parameters in the other three models are obtained from the best fit of the experimental data of bubble radii; (**e**) Temporal evolution of the number of air and vapor molecules inside the bubble predicted by our model; (**f**) The dimensionless pressure in the liquid during the first collapse stage.

References

1. Brennen, C.E. Cavitation in medicine. *Interface Focus* **2015**, *5*, 20150022.
2. Cui, P.; Zhang, A.M.; Wang, S.; Khoo, B.C. Ice breaking by a collapsing bubble. *Journal of Fluid Mechanics* **2018**, *841*, 287-309.
3. Brennen, C.E. *Cavitation and bubble dynamics*; Cambridge University Press, 2013.
4. Plesset, M.S.; Prosperetti, A. Bubble dynamics and cavitation. *Annu. Rev. Fluid Mech.* **1977**, *9*, 145-185.
5. Lauterborn, W.; Kurz, T. Physics of bubble oscillations. *Rep. Prog. Phys.* **2010**, *73*, 106501.
6. Fujikawa, S.; Akamatsu, T. Effects of the non-equilibrium condensation of vapor on the pressure wave produced by the collapse of a bubble in a liquid. *Journal of Fluid Mechanics* **1980**, *97*, 481512.
7. Yasui, K. Effects of thermal conduction on bubble dynamics near the sonoluminescence threshold. *J. Acoust. Soc. Am.* **1995**, *98*, 2772-2782.
8. Zhong, X.; Eshraghi, J.; Vlachos, P.; Dabiri, S.; Ardekani, A.M. A model for a laser-induced cavitation bubble. *International Journal of Multiphase Flow* **2020**, *132*, 103433.
9. Miles, P.R.; Smith, R.C. Parameter estimation using the python package pymcmcstat. Proc. of the 18th Python in Science Conf., Austin, USA, 2019.

* Corresponding Author: Arezoo M. Ardekani, ardekani@purdue.edu